

# Analytical design of densely dispersion-managed optical fiber transmission systems with Gaussian and raised cosine return-to-zero *Ansätze*

K. Nakkeeran, Y. H. C. Kwan, and P. K. A. Wai

*Photonics Research Center and Department of Electronic and Information Engineering,  
The Hong Kong Polytechnic University, Hung Hom, Kowloon, Hong Kong*

A. Labruyère, P. Tchofo Dinda, and A. B. Moubissi

*Laboratoire de Physique de l'Université de Bourgogne, B.P. 47 870, 21078 Dijon, France*

Received October 31, 2003; revised manuscript received May 25, 2004; accepted July 12, 2004

We propose an easy and efficient way to analytically design densely dispersion-managed fiber systems for ultrafast optical communications. This analytical design is based on the exact solution of the variational equations derived from the nonlinear Schrödinger equation by use of either a Gaussian or a raised-cosine (RC) *Ansatz*. For the input pulses of dispersion-managed optical fiber transmission systems we consider a RC profile and show that RC return-to-zero pulses are as effective as Gaussian pulses in high-speed (160-Gbits/s) long-distance transmissions. © 2004 Optical Society of America

*OCIS codes:* 060.5530, 060.2330, 060.4510, 190.5530.

## 1. INTRODUCTION

Dispersion-managed (DM) optical fiber systems have paved a new way to increase the transmitting capacity of optical fiber links.<sup>1–4</sup> Basically, the dispersion-management technique utilizes a fiber transmission line with a periodic dispersion map, such that each period is built up by two types of fiber, generally with different lengths and opposite group-velocity dispersion (GVD). In conventional DM fiber systems the length of the map is more than or equal to the amplifier span of the fiber transmission system.<sup>1</sup> But, because of large breathing and the large power-enhancement factor of these conventional DM solitons, it is difficult to propagate pulses with bit rates larger than 40 Gbits/s in each channel. Hence, to achieve pulse transmission at a high bit rate, Liang *et al.* proposed a densely dispersion-managed (DDM) fiber system whose dispersion map length is shorter than the amplifier span.<sup>5</sup>

Unlike for conventional solitons in uniform fibers, there is no exact analytical solution for DM solitons. Consequently, different methods for determining the parameters of stationary pulses (fixed points) for DM fiber lines have been developed, such as the averaging method of Nijhof *et al.*<sup>6</sup> and the numerical solution of the variational equations derived from the nonlinear Schrödinger equation (NLSE) by use of a Gaussian *Ansatz*.<sup>1</sup> Recently an analytical method for designing long-distance DM fiber lines was proposed by Nakkeeran *et al.*<sup>7</sup> Using that procedure,<sup>7</sup> one can easily design DM fiber transmission systems in the absence or presence of optical losses. In other words, this analytical design procedure permits one to obtain the length of the normal- and anomalous dispersion fiber sections for periodic evolution of a Gaussian pulse *Ansatz* (with desired width and energy) and any de-

sired fiber parameters (dispersion, nonlinearity, and losses). But that analytic design method<sup>7</sup> was strictly restricted to conventional DM fiber systems (i.e., with dispersion map lengths greater than or equal to one amplification period). Recently the use of average-dispersion-decreasing densely dispersion-managed (A4DM) fiber systems was proposed as an effective way to improve the performance of high-speed optical transmission systems.<sup>8</sup>

In all the studies mentioned above, a Gaussian profile for the pulse propagating in the DM fiber transmission line was assumed, whereas it is a known fact that pulses propagating in such systems are not exactly Gaussian pulses. In fact, it is its analytical tractability that makes the Gaussian *Ansatz* attractive, especially in the variational analysis of DM fiber systems. But, in practice, generating Gaussian profiled pulses at high bit rates is difficult. The output of the commonly used Mach-Zehnder modulators are raised-cosine (RC) profiled pulses. In general, developing ultrashort-pulse generators that facilitate both a high repetition rate and specific pulse profiles such as those that correspond to DM solitons remains a challenging technical problem. In this context it is natural to ask the following fundamental question: What is the level of tolerance of those transmission systems (designed on the basis of Gaussian pulses as approximate profiles of stationary pulses) with respect to variations in the input pulse profile? A related question is: What is the effect of pulse *Ansatz* when any other than the Gaussian profile is assumed in the design of the dispersion map?

To answer these questions we first consider a RC *Ansatz* as an approximate representation of the DM soliton. We derive the dynamic equations of the pulse parameters by using a collective-variable (CV) method.<sup>9</sup> From the

solution of the RC pulse parameter (width and chirp) equations we present an efficient analytical procedure for designing the dispersion map. For a particular example we show that the resultant analytically designed dispersion map from both the Gaussian and the RC *Ansätze* are almost the same and that an initial RC pulse executes similar kinds of dynamics in both dispersion maps. We then show that the RC return-to-zero pulses are as effective as the Gaussian pulses as input pulses in DM optical fiber transmission systems, which suggests the possibility of designing high-speed transmission lines that have high levels of tolerance with respect to variations in the input pulse profiles.

The paper is organized as follows: In Section 2 we consider the analytical design of an ideal transmission system without fiber losses, using both Gaussian and RC pulses as *Ansätze*, and derive the basic analytical formulas that give the fiber lengths of the dispersion map. We then study the propagation of these *Ansätze* in the analytically designed DM fiber systems. In Section 3 we exploit the basic formulas of the lossless system to derive analytical formulas for the DDM optical fiber transmission system including the fiber losses. In Section 4 we carry out numerical simulations that show that both the RC and the Gaussian input pulses can execute excellent transmissions at 160 Gbits/s over 6000 km in a transmission line designed analytically. We conclude with Section 5.

## 2. ANALYTICAL DESIGN OF THE LOSSLESS SYSTEM

Pulse dynamics in an ideal lossless DM fiber system are governed by the NLSE:

$$\psi_z + \frac{i\beta(z)}{2} \psi_{tt} - i\gamma(z)|\psi|^2\psi = 0, \quad (1)$$

where  $\psi$  is the slowly varying envelope of the axial electrical field and  $\beta(z)$  and  $\gamma(z)$  represent the GVD and the self-phase modulation parameters, respectively. We assume that the solution of the NLSE is in the form of either a Gaussian *Ansatz* ( $f_g$ ) or a RC *Ansatz* ( $f_{RC}$ ):

$$f_g = x_1 \exp\left(\frac{-t^2}{x_2^2} + \frac{ix_3 t^2}{2} + ix_4\right), \quad (2a)$$

$$f_{RC} = \frac{x_1}{2} \left[1 + \cos\left(\frac{\pi t}{x_2}\right)\right] \exp\left(\frac{ix_3 t^2}{2} + ix_4\right), \quad (2b)$$

where  $x_1$ ,  $x_3/(2\pi)$ , and  $x_4$  represent the pulse's amplitude, chirp, and phase, respectively. The full width at half-maximum (FWHM) intensity pulse width of the Gaussian and RC *Ansätze* are  $\sqrt{2 \ln 2} x_2$  and  $2x_2 \cos^{-1}(\sqrt{2} - 1)/\pi$ , respectively. Using a CV method,<sup>9</sup> we derive the following equations for the pulse width and chirp:

$$\dot{x}_2 = -\beta(z)x_2x_3, \quad (3a)$$

$$\dot{x}_3 = \beta(z) \left( x_3^2 - \frac{\alpha_1}{x_2^4} \right) - \frac{\alpha_2 \gamma(z) E_0}{x_2^3}, \quad (3b)$$

where the overdot represents the derivative with respect to  $z$  and the constants  $\alpha_j$  ( $j = 1, 2$ ) for Gaussian *Ansatz* (2a) are given by

$$\alpha_1 = 4, \quad \alpha_2 = \sqrt{2} \quad (4)$$

for the Gaussian *Ansatz* and

$$\alpha_1 = \frac{60\pi^4}{16\pi^4 - 600\pi^2 + 4545} \approx 32.2, \\ \alpha_2 = \frac{4375\pi^2}{48(16\pi^4 - 600\pi^2 + 4545)} \approx 4.9 \quad (5)$$

for the RC *Ansatz*.

In Eq. (3b),  $E_0 = x_1^2 x_2$  is a constant that is proportional to the pulse energy defined by  $E = \sqrt{\pi/2} E_0$  and  $E = (3/4)E_0$  for the Gaussian and RC *Ansätze*, respectively. Equations (3) are the more general form of Eqs. (3) reported earlier.<sup>7</sup> Hence, following the procedure presented by Nakkeeran *et al.*,<sup>7</sup> we derive a more-general expression for the lengths of normal ( $L_+$ ) and anomalous ( $L_-$ ) dispersion fiber sections of the dispersion map:

$$\frac{L_{\pm}}{2} = g(\beta_{\pm}, \gamma_{\pm}, c_{\pm}, x_{2\max}) - \frac{\alpha_2 \gamma_{\pm} \beta_{\pm} E_0}{2c_{\pm} \sqrt{2c_{\pm}}} \ln(4c_{\pm} x_{2\pm} - 2\alpha_2 \gamma_{\pm} \beta_{\pm} E_0), \quad (6)$$

where

$$g(\beta_{\pm}, \gamma_{\pm}, c_{\pm}, x_2) = \frac{\sqrt{R_{\pm}(x_2)}}{2c_{\pm}} + \frac{\alpha_2 \gamma_{\pm} \beta_{\pm} E_0}{2c_{\pm} \sqrt{2c_{\pm}}} \ln[2\sqrt{2c_{\pm} R_{\pm}(x_2)} + 4c_{\pm} x_2 - 2\alpha_2 \gamma_{\pm} \beta_{\pm} E_0], \\ R_{\pm}(x_2) = 2c_{\pm} x_2^2 - 2\alpha_2 \beta_{\pm} \gamma_{\pm} E_0 x_2 - \alpha_1 \beta_{\pm}^2, \\ c_{\pm} = \frac{\alpha_1 \beta_{\pm}^2}{2x_{2\pm}^2} + \frac{\alpha_2 \beta_{\pm} \gamma_{\pm} E_0}{x_{2\pm}}, \quad (7a) \\ x_{2\max} = \frac{\alpha_2 E_0 \beta_+ \beta_- (\gamma_+ \beta_- - \gamma_- \beta_+)}{c_+ \beta_-^2 - c_- \beta_+^2}. \quad (7b)$$

Here the GVD and self-phase modulation parameters for the two fiber segments are denoted  $\beta_{\pm}$  and  $\gamma_{\pm}$  (+ and - denote the normal and anomalous dispersion fibers), respectively. It is useful to present the different steps of

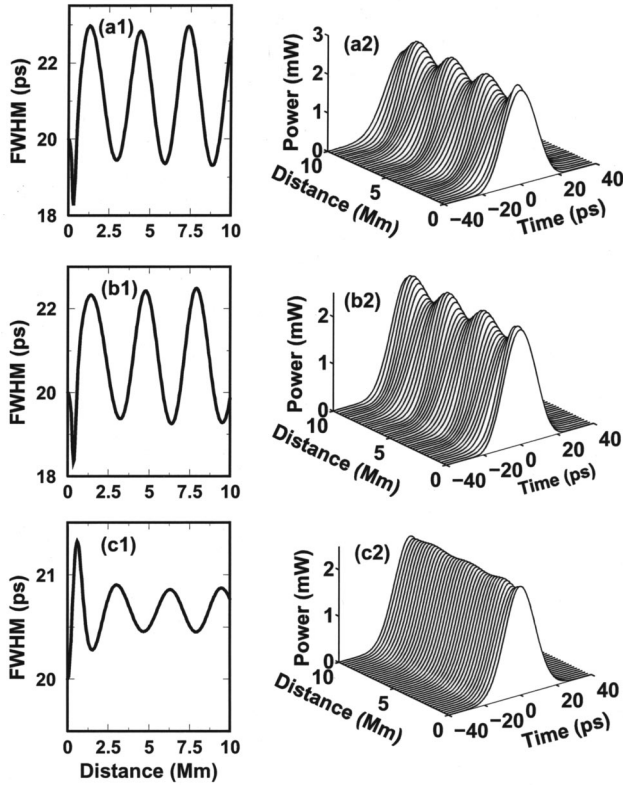


Fig. 1. Slow dynamics showing (a1), (a2) a RC pulse propagating in a DM fiber system designed by use of an RC *Ansatz*; (b1), (b2) a RC pulse propagating in a DM fiber system designed by use of a Gaussian *Ansatz*; (c1), (c2) a Gaussian pulse propagating in a DM fiber system designed by use of a Gaussian *Ansatz*.

the calculation procedure, using the above formulas for designing the dispersion map ( $L_-/2, L_+, L_-/2$ ) for any desired pulse and fiber parameters. We consider the beginning point of the DM fiber line as the midpoint of the anomalous dispersion fiber. In our analytical design we need the following five parameters:  $x_{2-}$ ,  $E_0$ ,  $\beta_{\pm}$ ,  $\gamma_{\pm}$ , and  $x_{2\max}$ , as input data. Using the first four parameters, we calculate the constant  $c_-$  from Eq. (7a). Then for calculating  $c_+$  we use the input datum  $x_{2\max}$  in Eq. (7b). Next we calculate the value of  $x_{2+}$ , using Eq. (7a). Finally, using Eqs. (6), we can straightforwardly evaluate the lengths of the normal and anomalous dispersion fiber sections of the dispersion map, which are required for the periodic evolution of any desired pulse (width and energy) and fiber (GVD and self-phase modulation) parameters.

To compare the dynamics of the Gaussian and RC *Ansätze*, one may consider the same energy and FWHM for both the Gaussian and the RC pulses as the input pulse parameters in our analytical design. With the following typical input data: initial FWHM, 20 ps; energy,  $E = 0.05$  pJ; maximum FWHM, 33 ps; breathing factor,<sup>10</sup>  $x_{2\max}/x_{2-} = 1.65$ ;  $\beta_{\pm} = \pm 15.9$  ps<sup>2</sup> km<sup>-1</sup>; and  $\gamma_{\pm} = 0.002$  m<sup>-1</sup> W<sup>-1</sup>, we directly obtain  $L_- = 24.16$  km, and  $L_+ = 23.55$  km for the Gaussian *Ansatz* and  $L_- = 22.35$  km and  $L_+ = 21.69$  km for the RC *Ansatz*. We find that the dispersion maps designed with the Gaussian and the RC *Ansätze* are essentially of the same order for Gaussian and RC pulses propagating with the same energy and FWHM. It is useful to solve the NLSE to inves-

tigate the propagation of these *Ansätze* in the analytically designed DM fiber systems. Figure 1 shows the slow dynamics of the pulse when a RC pulse propagates in the DM fiber system designed with the RC *Ansatz* [Figs. 1(a1) and 1(a2)], when a RC pulse propagates in the system designed with the Gaussian *Ansatz* [Figs. 1(b1) and 1(b2)], and when a Gaussian pulse propagates in the system designed with the Gaussian *Ansatz* [Figs. 1(c1) and 1(c2)]. One can clearly observe that the initially RC pulse executes essentially the same dynamic behavior in the two DM fiber systems designed with the RC *Ansatz* [Figs. 1(a1) and 1(a2)] and the Gaussian *Ansatz* [Figs. 1(b1) and 1(b2)]. Also, we can observe from Figs. 1(b1) and 1(c1) that the initially RC and Gaussian pulses execute slow dynamics with different magnitudes but at the same average pulse width,  $\approx 20.75$  ps. Furthermore, we can observe from Figs. 1(c1) and 1(c2) that the slow dynamics of the initially Gaussian pulse propagation execute lesser variations than for the RC pulse, thus indicating that the Gaussian *Ansatz* provides a better approximation for the profile of a DM soliton in the lossless DM fiber system than does the RC *Ansatz*. Here the important fact to be noted is the similar kind of slow dynamics executed by the initial RC pulse in both dispersion maps designed by use of the Gaussian and the RC *Ansätze*.

It is interesting, however, to compare the fast dynamics for the two types of pulse within one dispersion map. Considering the analytically designed DM fiber systems with the Gaussian and RC *Ansätze* described above, we solved pulse dynamic equations (3) with the initial conditions derived from the fixed-point solutions of the respective dispersion maps. Figure 2 shows the evolution of pulse width and chirp within one dispersion map designed by use of the RC [Figs. 2(a1) and 2(b1)] and the Gaussian [Figs. 2(a2) and 2(b2)] *Ansätze*, respectively. Solid, dashed, and dotted curves show the solutions of RC *Ansatz* dynamic equations (3) with (5), Gaussian *Ansatz* equations (3) with (4), and the NLSE (1), respectively. We have obtained the pulse parameters from the exact numerical solution of the NLSE (dotted curves in Fig. 2)

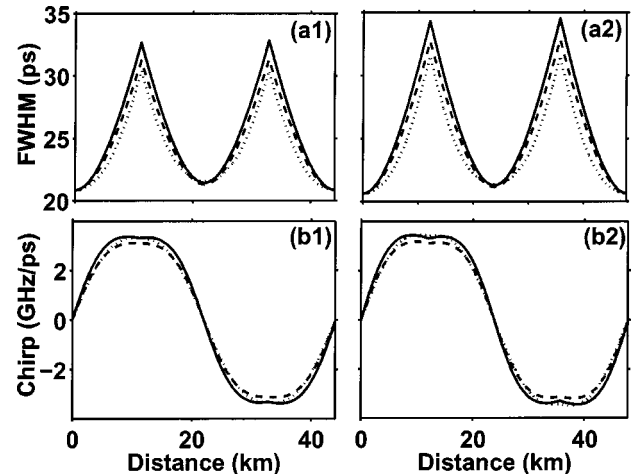


Fig. 2. Evolution of pulse width and chirp in one dispersion map designed by use of (a1), (b1) a RC *Ansatz* and (a2), (b2) a Gaussian *Ansatz*. Solid, dashed, and dotted curves show the solutions of RC *Ansatz* dynamic equations (3) with (5), Gaussian *Ansatz* equations (3) with (4) and NLSE (1), respectively.

by means of a CV method<sup>9</sup> that we briefly describe in Section 3 below. From the results we can clearly see that pulse evolution calculated from the solutions of the RC *Ansatz* dynamic equations is essentially the same as the solutions of the Gaussian *Ansatz* equations. Also, the solutions of both RC and Gaussian *Ansätze* dynamic equations are similar to the exact numerical solution of the NLSE [Eq. (1)]. Consequently we conclude that the RC return-to-zero pulse executes essentially the same dynamic behavior as the Gaussian pulse in the lossless DM fiber system.

Thus it follows from the general qualitative considerations stated above that isolated pulses originating from RC and Gaussian input pulses that have the same energy and the same width will execute similar dynamic behaviors in the phase space of a lossless DM fiber system. We show in Section 3 below that, in the real transmission line with losses and periodic amplification, to achieve excellent transmissions there is no need for the RC and Gaussian input pulses to have the same width. Indeed, through remarkable reshaping, RC and Gaussian pulses with different initial widths can be transformed while they are propagating until they ultimately converge toward the same parameter region of high stability in phase space, as we show below.

### 3. ANALYTICAL DESIGN OF THE LOSSY SYSTEM

A fundamental property of DM solitons in a lossless DM fiber system lies in the close relationship between the pulse energy and the average dispersion.<sup>11–14</sup> The higher the magnitude of the average dispersion, the higher the energy of stationary pulses.<sup>11–14</sup> A real DM fiber line contains optical losses, which cause the pulse energy to decrease exponentially along each amplification span. Before the novel idea of dispersion compensation arose, researchers were trying to design a dispersion-decreasing fiber system to counterbalance the decreasing nonlinearity (which was due to optical losses).<sup>15–17</sup> But the difficulty of fabricating such types of fiber has prevented this concept from becoming a reality. However, in accordance with this concept, A4DM fiber systems were recently proposed as an effective way to improve the performance of high-speed optical transmission systems.<sup>8,18</sup> The A4DM fiber systems correspond to DDM lines that have decreasing average dispersion from one map to another within each amplification period. The basic idea of our analytical design of the lossy system is similar to that of A4DM fiber systems. That is, the idea is to divide the amplification span into several pieces and to treat the pieces as lossless subsystems like those that were considered in Section 2 but with exponentially decreasing energies from one subsystem to the next.<sup>8,18</sup> In other words, we treat every dispersion map within the amplification span as a lossless subsystem that is designed in a such way that its average dispersion is closely related to the energy that the pulse will have in that map. Thus, following this idea, we can carry out the design of an A4DM fiber system through the following simple procedure for constructing any number ( $N$ ) of dispersion maps in one amplification period:

$$L_{n-} = \frac{\left[ \beta_{a1} \exp\left(-\sum_{i=1}^{n-1} T_i\right) - \beta_+\right] L}{\beta_- - \beta_+} \quad (8)$$

for  $n = 2, \dots, N$ , where  $T_i$  designates the total losses in the  $i$ th map and  $L$  is the dispersion map length. Note that, in the presence of fiber losses only,  $T_i = \alpha_+ L_{i+} + \alpha_- L_{i-}$ , where  $\alpha_{\pm}$  are the loss parameters for the two types of fiber. The parameter  $\beta_{a1} = (\beta_+ L_{1+} + \beta_- L_{1-}) / (L_{1+} + L_{1-})$  represents the average dispersion of the first dispersion map.

In what follows, we show that Gaussian and RC pulses can execute long-distance and highly stable propagation in a much simpler line than in the A4DM fiber system, that is, a DDM fiber line in which each amplification span is made up of a repetition of a single type of map. This simple DDM fiber line possesses a constant average dispersion, say,  $\beta_m$ , that corresponds to the span's average dispersion of an equivalent A4DM fiber system.<sup>19</sup> Therefore we have

$$\beta_m = \frac{\beta_{a1}}{T} [1 - \exp(-T)], \quad T = \sum_{i=1}^{N-1} T_i. \quad (9)$$

Then, with knowledge of  $\beta_m$  and map length  $L$ , we can immediately calculate the fiber lengths of the dispersion map ( $\mathcal{L}_{\pm}$ ) of the DDM fiber line:

$$\mathcal{L}_+ = \left( \frac{\beta_m - \beta_-}{\beta_+ - \beta_-} \right) L, \quad \mathcal{L}_- = L - \mathcal{L}_+. \quad (10)$$

Thus the DDM fiber system is designed by a fully analytical procedure with two steps: First, one must design the equivalent A4DM fiber line for the desired pulse and fiber parameters. Second, using Eqs. (9) and (10), one can calculate fiber lengths  $\mathcal{L}_-$  and  $\mathcal{L}_+$ .

### 4. NUMERICAL SIMULATIONS

To illustrate the effectiveness of RC pulses we have considered pulse propagation in a single channel line operating at 160 Gbits/s. Using the above analytical procedure on the basis of a Gaussian *Ansatz*, we designed a DDM fiber system with an amplification span of  $Z_A = 25$  km, a symmetric dispersion map made up of an alternating juxtaposition of teralight and reverse teralight fibers, and the following parameters (in anomalous dispersion fiber: in normal dispersion fiber): second-order dispersion  $\beta_{\mp} = [8 \text{ (ps/nm)/km} : -16 \text{ (ps/nm)/km}]$ ; third-order dispersion  $[0.06 \text{ (ps/nm}^2\text{)/km} : -0.12 \text{ (ps/nm}^2\text{)/km}]$ ; effective core area ( $60 \mu\text{m}^2 : 25 \mu\text{m}^2$ ); losses  $\alpha_{\mp} = (0.2 \text{ dB/km} : 0.28 \text{ dB/km})$ ; amplifier noise figure, 4.5 dB; and Gaussian filters of bandwidth 1.4 THz (placed in line at each amplifier site) to reduce the timing jitter. In these numerical simulations we have not included the effects of stimulated Raman scattering and polarization mode dispersion. For the simulations we solved the NLSE including the higher-order effects mentioned above. To evaluate the transmission performances, we use a standard approach in which one assumes Gaussian probability-density functions for the input voltage to the decision circuit for both the 0 and the 1 levels. Then one

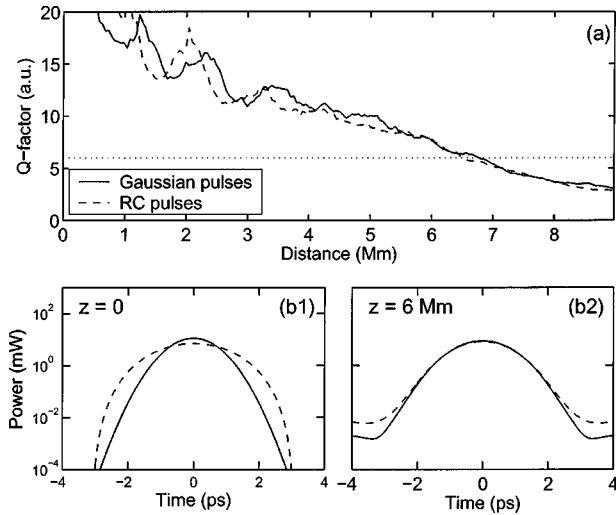


Fig. 3. (a)  $Q$  factor versus propagation distance  $z$ , showing the transmission performance of 128-bit pseudorandom binary sequence patterns of initially Gaussian pulses and initially RC pulses, in our analytically designed DDM fiber line. The  $Q$  factor is given in linear units, and the dotted line represents  $Q = 6$ . (b1) Profiles of the input pulses used in the transmission. (b2) Profiles of the output pulses after single-pulse transmission. Solid and dashed curves in (b1) and (b2) correspond to initially Gaussian and RC profiles, respectively.

evaluates the  $Q$  factor from the mean values  $\mu_0$  and  $\mu_1$ , and the standard deviations  $\sigma_0$  and  $\sigma_1$  of the 0 and 1 levels, respectively. Here the amplitude  $Q$  factor, which serves as a measure of the amplitude jitter, is defined by  $Q_A \equiv (\mu_1 - \mu_0)/(\sigma_1 + \sigma_0)$ , whereas timing  $Q$  factor serves as a measure of the timing jitter and is defined by  $Q_T \equiv 0.7T_d/\sigma_T$ , where  $T_d = 6.25$  ps is the size of the bit slot and  $\sigma_T$  is the standard deviation of the 1 with respect to the center of the bit slot. We define the transmission distance,  $L_{\max}$ , as the maximum distance over which the smaller of the two  $Q$  factors,  $\min(Q_A, Q_T)$ , remains higher than 6. Note that here the  $Q$  factor is given in linear units. The value  $Q = 6$  corresponds to a bit-error ratio of  $10^{-9}$ . To obtain a fair evaluation of the system's performance we carried out two series of simulations that corresponded to Gaussian and RC input pulses. For the first series of simulations, the input (chirp-free) pulse was chosen to be a Gaussian pulse with width  $x_2 = 1.18$  ps, maximum pulse width  $x_{2\max} = 2.24$  ps, and energy  $E = 0.0165$  pJ. For the second series of simulations we used RC input (chirp-free) pulses with  $x_2 = 3.125$  ps and same energy as for the Gaussian pulses ( $E = 0.0165$  pJ). The DDM fiber transmission line was designed by use of analytical formulas (6), (8), and (10) for a Gaussian *Ansatz*. Hence we obtained the following fiber lengths for the dispersion map:  $\mathcal{L}_- = 220.53$  m and  $\mathcal{L}_+ = 110.20$  m. The solid and dashed curves in Fig. 3(a) show the transmission performance of 128-bit pseudorandom binary sequence patterns of Gaussian and RC input pulses, respectively. The horizontal dotted line represents  $Q = 6$ . This figure demonstrates, as a general feature, a relatively high stability of the initially Gaussian and RC pulses, with similar performance over several thousands of kilometers ( $L_{\max} > 6$  Mm). Hence the remarkable fact is that similar

performance is obtained with pulses that have the same energy ( $E = 0.0165$  pJ) but quite different profiles, as can be seen from Fig. 3(b1), which shows the profiles of the Gaussian input pulse (solid curve) and of the RC input pulse (dashed curve). Furthermore, Fig. 3(b2), which shows the profiles of the initially Gaussian pulse (solid curve) and of the initially RC input pulse (dashed curve) after a propagation distance of 6000 km, reveals that the two types of pulse are transformed while they propagate and converge toward the same stationary profile.

Thus the results in Fig. 3 reveal a particularly interesting property of our DDM fiber system, that is, a certain tolerance of the system with respect to variation of pulse shape, facilitating excellent transmissions over transoceanic distances for initially Gaussian pulses as well as for RC pulses on the same line. As this property of DM solitons has been largely neglected in previous studies, a question arises: To what can one attribute this robustness of the DDM fiber line with respect to such a variation of input pulse profile?

One can gain some insight into this issue by examining the dynamic behavior of isolated RC and Gaussian pulses in the DDM fiber line under consideration. In this context, we have found that filters play a major role in the high stability of the RC and Gaussian pulses. Indeed, we have used a CV approach<sup>9</sup> to the dynamics of an isolated pulse by explicitly taking into account the residual field.

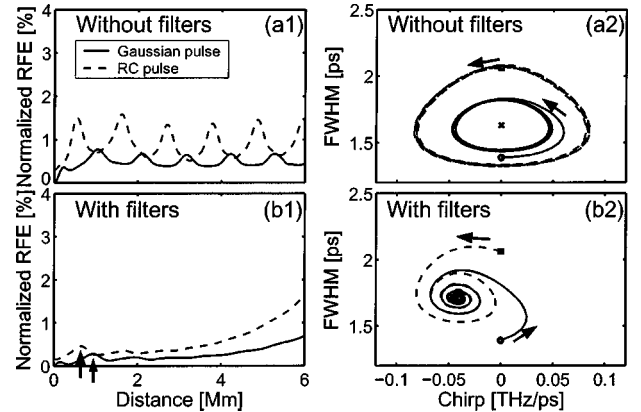


Fig. 4. Collective-variable analysis by use of the Gaussian *Ansatz* for single-pulse propagation in the DDM fiber line.

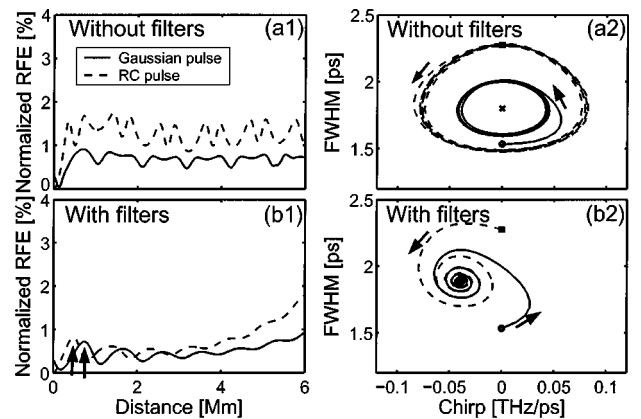


Fig. 5. Collective-variable analysis by use of the RC *Ansatz* for single-pulse propagation in the DDM fiber line.

In this approach one decomposes the soliton field (exact solution of the generalized NLSE modeling the DDM fiber transmission line) in the following way:<sup>9</sup>

$$\psi(z, t) = f(x_1, x_2, x_3, x_4, t) + q(z, t), \quad (11)$$

where *Ansatz* function  $f$  is chosen to be either the Gaussian ( $f_g$ ) or the RC ( $f_{RC}$ ) *Ansatz*, values of  $x_j$  designate the pulse parameters, and  $q$  is the remaining field such that the sum of  $f$  and  $q$  satisfies the generalized NLSE. This field  $q$ , called the residual field, accounts for the dressing of the soliton and any radiation coupled to the soliton's motion. By knowing the exact field  $\psi(z, t)$ , from numerical solution of the generalized NLSE one can obtain the soliton parameter at each distance  $z$  through minimization of the residual field energy (RFE).<sup>9</sup> Following this CV procedure, first with a Gaussian *Ansatz* ( $f = f_g$ ) and then with a RC *Ansatz* ( $f = f_{RC}$ ), we obtained the results presented in Figs. 4 and 5, respectively. These figures represent the slow dynamics of an isolated pulse. A careful inspection of Figs. 4 and 5 reveals the following properties:

(i) One can clearly observe that, whether one injects Gaussian pulses (solid curves) or RC pulses (dashed curves), the procedure of minimization of the RFE always ends up with a nonzero RFE, as can be seen from Figs. 4(a1) and 4(b1) and Figs. 5(a1) and 5(b1). A nonzero RFE demonstrates that, whether one injects Gaussian or RC pulses, the pulses that propagate in the line do not correspond either to Gaussian pulses or to RC pulses. Hence, as soon as they are injected in the line, the initially Gaussian (or RC) pulses execute a reshaping process in which they lose their initial profiles and acquire specific profiles, say,  $\psi_g$  (or  $\psi_{RC}$ ), which depend strongly on the line parameters (amplification span, dispersion map, types of fiber, amplifiers). For simplicity, pulses  $\psi_g$  and  $\psi_{RC}$  hereafter are referred to as DDM soliton.

(ii) One can gain some insight into the behavior of  $\psi_g$  by comparing the associated RFEs. A comparison of the solid curves in Figs. 4(a1) and 5(a1) reveals essentially equivalent RFEs. This indicates that, in the absence of filters, initial Gaussian pulses lead to DDM solitons that are not any closer to Gaussian profiles than to RC profiles. In the presence of Gaussian filters, the profile of the DDM soliton becomes slightly closer to a Gaussian profile than to a RC profile, as the solid curves in Fig. 4(b1) and Fig. 5(b1) show.

(iii) A comparison of the dashed curve in Fig. 4(a1) [4(b1)] with that in Fig. 5(a1) [5(b1)] reveals that, whether or not the filters are present in the line, the input RC pulses lead to DDM solitons  $\psi_{RC}$  that are not any closer to a RC profile than to a Gaussian profile.

(iv) We can achieve a direct comparison of  $\psi_g$  and  $\psi_{RC}$  by comparing the solid and dashed curves in each of Figs. 4(a1), 4(b1), 5(a1), and 5(b1). In all cases the initially Gaussian pulses  $\psi_g$  lead to a RFE (solid curve) that is smaller than that which corresponds to the  $\psi_{RC}$  pulses (dashed curves). This clearly indicates that soliton  $\psi_g$  radiates away less energy than soliton  $\psi_{RC}$  during propagation in the transmission line. Although this radiative process can be detrimental to the stability of the pulses, its effects can be counterbalanced by a filtering action, as we explain below.

Figures 4(a2) and 5(a2) demonstrate that filters play a crucial role in the stabilization of both  $\psi_g$  and  $\psi_{RC}$  solitons, with an increased benefit for initially RC pulses  $\psi_{RC}$ . Figure 4(b1), which shows the evolution of chirp and FWHM of the pulse in the phase plane, shows that in the absence of filters each of the DDM solitons executes essentially a periodic slow dynamics, in which the pulse periodically returns back toward its initial condition. Furthermore, Fig. 4(a1) shows that the RFE executes variations with a mean value that does not increase with distance. These two properties reflect the possibility of infinite propagation of an isolated (initially Gaussian or RC) pulse in the line, and therefore, illustrate the fact that our analytically designed DDM fiber line ensures fundamental stabilization quite well by causing the pulse to execute closed-loop trajectories about the fixed point of the line (represented by the small cross in the figure). It is worth noting that the evaluations of the fixed point made by the CV approach with the Gaussian *Ansatz* [Fig. 4(a2)] and the CV approach with the RC *Ansatz* [Fig. 5(a2)] are slightly different because of perturbed environmental conditions (i.e., the presence of a nonzero residual field). Nevertheless, both the Gaussian and the RC *Ansätze* lead to a fixed point with  $1.6 \text{ ps} < \text{FWHM} < 1.8 \text{ ps}$  and a chirp of approximately 0. But the most important point to be emphasized here is that, in the absence of filters, isolated soliton  $\psi_{RC}$  executes larger variations of its width than does  $\psi_g$  soliton with same energy [as Fig. 4(a2) shows]. This result indicates that soliton  $\psi_{RC}$  will be more prone to interactions between adjacent pulses if a pulse train is transmitted in a DDM fiber line without filters. Now Figs. 4(b2) and 5(b2) exhibit an important virtue of Gaussian filters, which is that they induce a strong reduction of the range of variation of the pulse width about the fixed point. In general we observe from Figs. 4(b2) and 5(b2) two outstanding steps in the pulse dynamics. In the first step the pulse continually moves away from its initial condition under the filter's action, until it reaches a small parameter region close to the fixed point. Then the pulse enters the second step, in which it executes an oscillatory internal motion with decreasingly small variations of the pulse width about the fixed point. From a more fundamental point of view, Figs. 4(b1) and 5(b1) reveal the presence of a large peak (indicated by the upward-pointing arrows) in the RFE. This peak results from a strong reshaping process that takes place in the first step of the dynamics, in which the pulse is transformed into a DDM soliton. This reshaping process is accompanied by a strong radiation of energy away from the pulse; hence the large initial peak in the RFE. This peak is much larger for soliton  $\psi_{RC}$  than for  $\psi_g$  [as the dashed curves in Figs. 4(b1) and 5(b1) show]. In the second step of the dynamics the reshaping process continues but in smooth manner, and there the RFE increases with distance in a smooth manner also.

Finally, the most important result of the CV analysis above is given in Figs. 4(b2) and 5(b2), which show that the combined action of our analytically designed DDM fiber line with in-line Gaussian filters forces the initially RC pulses to evolve within a relatively small parameter region close to the fixed point of the transmission line, which is essentially the same as that of initially Gaussian

pulses with the same energy. This increased proximity with respect to the fixed point reinforces the pulse stability against the radiation that results from the pulse reshaping. These processes explain why RC pulses can be as effective as Gaussian pulses in long-distance transmissions through DDM fiber lines.

## 5. CONCLUSIONS

To conclude, we have presented an easy and efficient way to analytically design DDM fiber systems by using the explicit solution of pulse dynamic equations of both RC and Gaussian *Ansätze*. As the initial RC pulse executes similar kinds of dynamics in dispersion maps designed with both Gaussian and RC *Ansätze*, one can effectively use the RC pulse as the initial profile for the dispersion map, analytically designed by use of the Gaussian ansatz.

One major issue in upgrading the existing transmission systems or designing new systems, however, lies in the difficulty of developing ultrashort pulse generators to produce both high repetition rates and pulse profiles of high quality. In this context, the tolerance of transmission systems with respect to pulse shape will become an increasingly important issue in the development of future fiber-optic links. The results obtained here represent a step forward in overcoming this problem. Using our analytical design procedures, we have shown that RC pulses are as effective as Gaussian pulses in DDM optical fiber systems designed for Gaussian pulses. Hence the output of the Mach-Zehnder modulators can be effectively utilized as the initial pulses for the return-to-zero encoded transmission in DM fiber systems.

## ACKNOWLEDGMENTS

This research is supported by The Hong Kong Polytechnic University (project G-YW85). We gratefully acknowledge partial support of this research by the Center National de la Recherche Scientifique and the Ministère de l'Éducation Nationale de la Recherche et de la Technologie, France.

K. Nakkeeran's e-mail address is ennaks@polyu.edu.hk.

## REFERENCES

1. V. E. Zakharov and S. Wabnitz, *Optical Solitons: Theoretical Challenges and Industrial Perspectives* (Springer-Verlag, Berlin, 1998).
2. M. Nakazawa, H. Kubota, K. Suzuki, E. Yamada, and A. Sahara, "Recent progress in soliton transmission technology," *Chaos* **10**, 486–514 (2000).
3. A. Maruta, Y. Yamamoto, S. Okamoto, A. Suzuki, T. Morita, A. Agata, and A. Hasegawa, "Effectiveness of densely dispersion managed solitons in ultra-high speed transmission," *Electron. Lett.* **36**, 1947–1949 (2000).
4. L. J. Richardson, W. Forysiak, and N. J. Doran, "Transoceanic 160-Gbit/s single-channel transmission using short-period dispersion management," *IEEE Photonics Technol. Lett.* **13**, 209–211 (2001).
5. A. H. Liang, H. Toda, and A. Hasegawa, "High-speed soliton transmission in dense periodic fibers," *Opt. Lett.* **24**, 799–801 (1999).
6. J. H. B. Nijhof, N. J. Doran, W. Forysiak, and F. M. Knox, "Stable soliton-like propagation in dispersion managed systems with net anomalous, zero and normal dispersion," *Electron. Lett.* **33**, 1726–1727 (1997).
7. K. Nakkeeran, A. B. Moubissi, P. Tchofo Dinda, and S. Wabnitz, "Analytical method for designing dispersion-managed fiber systems," *Opt. Lett.* **26**, 1544–1546 (2001).
8. A. B. Moubissi, K. Nakkeeran, P. Tchofo Dinda, and S. Wabnitz, "Average dispersion decreasing densely dispersion-managed fiber transmission systems," *IEEE Photonics Technol. Lett.* **14**, 1279–1281 (2002).
9. P. Tchofo Dinda, A. B. Moubissi, and K. Nakkeeran, "Collective variable theory for solitons in optical fibers," *Phys. Rev. E* **64**, 016608 (2001).
10. K. Nakkeeran, A. B. Moubissi, and P. Tchofo Dinda, "Analytical design of dispersion-managed fiber system with map strength 1.65," *Phys. Lett. A* **308**, 417–425 (2003).
11. A. Berntson, N. J. Doran, W. Forysiak, and J. H. B. Nijhof, "Power dependence of dispersion-managed solitons for anomalous, zero, and normal path-average dispersion," *Opt. Lett.* **23**, 900–902 (1998).
12. T. Yu, E. A. Golovchenko, A. N. Pilipetskii, and C. R. Menyuk, "Dispersion-managed soliton interactions in optical fibers," *Opt. Lett.* **22**, 793–795 (1997).
13. B. A. Malomed, "Suppression of soliton jitter and interactions by means of dispersion management," *Opt. Commun.* **147**, 157–162 (1998).
14. M. Zitelli, B. Malomed, F. Matera, and M. Settembre, "Strong time jitter reduction using solitons in '1/z' dispersion managed fiber links," *Opt. Commun.* **154**, 273–276 (1998).
15. A. J. Stentz, R. W. Boyd, and A. F. Evans, "Dramatically improved transmission of ultrashort solitons through 40 km of dispersion-decreasing fiber," *Opt. Lett.* **20**, 1770–1772 (1995).
16. S. Kawai, K. I. Suzuki, and K. Iwatsuki, "Ultra-high speed long distance nonlinear waveform reshaping transmission using adiabatic soliton compression and narrowband sliding-frequency filter," *Electron. Lett.* **32**, 2170–2171 (1996).
17. T. Georges and B. Charbonnier, "Continuum generated by chromatic dispersion and power variations in periodically amplified soliton links," *Opt. Lett.* **21**, 1232–1234 (1996).
18. P. Tchofo Dinda, A. Labruière, K. Nakkeeran, J. Fatome, A. B. Moubissi, S. Pitois, and G. Millot, "On the designing of densely dispersion-managed optical fiber systems for ultrafast optical communication," *Ann. Telecommun.* **58**, 1785–1808 (2003).
19. A. Labruière, P. Tchofo Dinda, K. Nakkeeran, and A. B. Moubissi, "Feasibility of  $N \times 160$  Gbit/s ultra-long haul transmissions in densely dispersion-managed optical fiber systems," submitted to *Opt. Commun.*